Journal of Molecular Catalysis A: Chemical 315 (2010) 148–154

Contents lists available at ScienceDirect

Journal of Molecular Catalysis A: Chemical

journal homepage: www.elsevier.com/locate/molcata

Kinetic modelling of regioselectivity in alkenes hydroformylation over rhodium

Dmitry Yu. Murzin*, Andreas Bernas, Tapio Salmi

Åbo Akademi University, Biskopsgatan 8, 20500 Turku/Åbo, Finland

ARTICLE INFO

Article history:
Available online 30 June 2009

Dedicated to 100th anniversary of Prof. M.I. Temkin.

Keywords:
Hydroformylation
Alkene
Rhodium
Regioselectivity
Modelling

ABSTRACT

Propene hydroformylation was performed with rhodium triphenylphosphine catalyst with hydrogen and CO partial pressure varied in the range of 8–15 bar. The regioselectivity was independent on the concentration of reactants, displaying dependence only on the ligand concentration. A kinetic model was proposed based on the mechanism of alkene hydroformylation and compared with experimental observations. Numerical data fitting was performed showing good correspondence of reaction rates and regioselectivity with experimental data.

© 2009 Elsevier B.V. All rights reserved.

1. Introduction

Homogeneous catalysis by metal complexes, widely utilized in academic research, also made its way into industry. One of the most prominent examples of applied homogeneous catalysis is hydroformylation, or oxo-synthesis, which is an important industrial process for the production of aldehydes from alkenes (Fig. 1) [1,2].

One of the commonly studied catalysts for this reaction is $HRh(CO)(PPh_3)_3$. The currently accepted mechanism for Rh/PPh_3 hydroformylation is shown in Fig. 2 [3]. Usually only one cycle is discussed, and mechanistic aspects of regioselectivity are rather seldom addressed [4].

The regioselectivity (e.g. the selectivity to linear over branched aldehydes) can be very high reaching routinely 70–92% and even a linear to branch ratio of 500 was attained depending on temperature, ligand concentration and hydrogen to CO ratio [1,2]. In industrial conditions excess of phosphine ligand is used, although activity is deteriorated, but selectivity towards linear aldehyde is improved.

The addition of excess phosphine ligand shifts the phosphine dissociation equilibrium towards the more selective $HRh(CO)(PPh_3)_2$ catalyst. Although it is reported sometimes in the literature that higher CO partial pressures lower the product linearity, our recent experimental data [5] obtained in the pressure range of synthesis gas below 15 bar showed independence of selectivity from CO. However, the regioselectivity of $HRh(CO)(PPh_3)_2$ was seen to be dependent on the concentration of PPh_3 as the following rate equations were found to be adequate to explain experimental data

$$r_i = k_i C_{alkene} C_{H_2} C_{CO} C_{Rh} C_{PPh_3}^{-0.54} \quad (1)$$

$$r_n = k_n C_{alkene} C_{H_2} C_{CO} C_{Rh} C_{PPh_3}^{-0.30} \quad (2)$$

and subsequently

$$\frac{r_n}{r_i} = \frac{k_n}{k_i C_{PPh_3}^{0.16}} \quad (3)$$

where r_n and r_i correspond to formation of linear and branched aldehydes, respectively.

Despite the industrial importance of hydroformylation reaction and substantial amount of research devoted to understanding the mechanism of this reaction, there are only a few kinetic studies where the kinetic equations are derived from mechanistic considerations and compared with experimental observations. In our previous contribution [5] only a simple kinetic model of power law type has been applied. In this paper, a mechanistic and more extended kinetic model is evaluated.

The aim of this contribution is to discuss the mechanism of hydroformylation and to compare the kinetics, which corresponds to the mechanism, with experimental observations, focusing mainly on regioselectivity. The theory of complex reac-

* Corresponding author. Tel.: +358 2 215 4985.
E-mail address: dmurzin@abo.fi (D.Yu. Murzin).

1381-1169/$ – see front matter © 2009 Elsevier B.V. All rights reserved.
doi:10.1016/j.molcata.2009.06.023

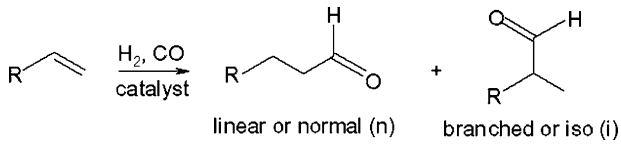

Fig. 1. Hydroformylation of alkenes.

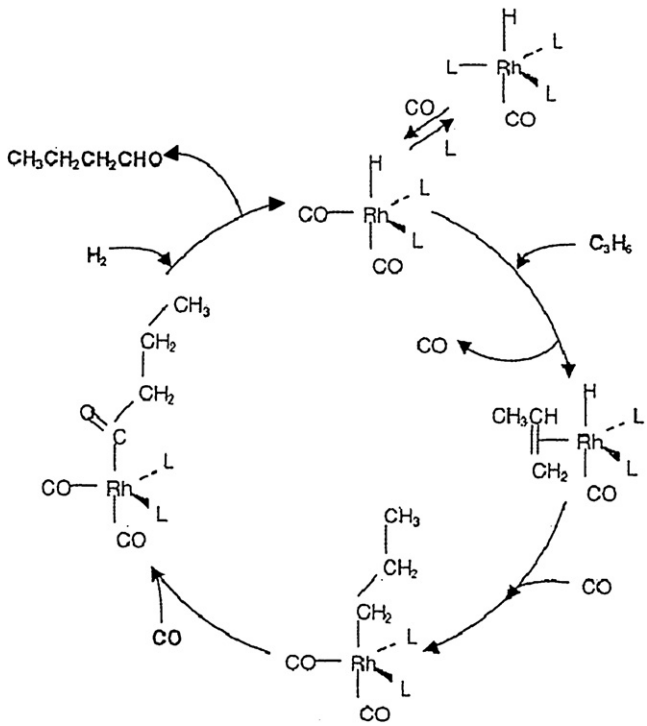

Fig. 2. Hydroformylation mechanism [3].

tions with the notions of reaction routes, developed by Temkin [6] will serve as a tool.

2. Experiment procedure

The experiments were carried out in a stirred and pressurized 300-ml reactor made of stainless steel (Parr 4561). It had an internal cooling loop and was equipped with an automatic temperature control system consisting of an external electric heating jacket coupled to a steering unit (Parr 4843), which was also used to control the stirring speed. The temperature could be maintained within ±1 °C. The reactor had facilities for sampling of the liquid phase as well as the gaseous content. The reactor was connected to reservoirs of alkene and nitrogen. Synthesis gas containing H_2/CO mixtures could be fed at a constant pressure to the reactor by means of a pressure regulator (Brooks 5866, Brooks 0154) and the reactor was equipped with transducers for on-line measurements of pressure (Keller Type PA21 SR/80520.3-1) and temperature which was followed up on a PC for continuous data logging.

The catalyst precursor and the ligand were dissolved in 2,2,4-trimethyl-1,3-pentanediol monoisobutyrate. The solution was charged into the steel reactor. The reactor was sealed tight and the heating jacket was attached. The gases fed into the reactor were dispersed in the liquid phase by the aid of a sinter. Propene was flushed though the liquid phase at the flow rate of 22 l/h for 7 min at 1.2 bar and room temperature. The reactor was kept closed for 25 min to await gas–liquid equilibrium. The reactor was heated to the reaction temperature of 70–115 °C while the total pressure increased to ~6 bar. After stabilization of the temperature, a zero sample was taken from the liquid phase. The stirring was kept on during this entire procedure. The reaction time was initialized to zero as soon as the reactor was pressurized with hydrogen–carbon monoxide syngas. Samples of the volume 1 ml were taken from the liquid phase.

3. Reaction mechanism

It is generally accepted that the active catalyst form is a four-coordinated intermediate like $HRh(CO)(PPh_3)_2$. According to [1] the catalytic cycle with this intermediate gives only predominantly linear aldehyde. Such an intermediate can undergo transformations, leaving one ligand and accepting one CO molecule. Monophosphine complexes are not selective giving an equimolar mixture of linear and branched aldehydes. The mechanism, presented in Fig. 3 should in principle give dependence of regioselectivity on the CO pressure and triphenylphosphine concentration.

Experimental data, generated in [5], show no dependence of regioselectivity on the CO concentration within the studied range of conditions, which imposes some restrictions on the transformations between RhHLCO and $RhHL_2CO$. It is supposed that the cycle where $RhHL_2CO$ is involved leads to a higher amount of linear aldehyde, while the cycle with RhHLCO is not regioselective, in the extreme case giving an equimolar ratio of linear and branched aldehyde.

The reaction mechanism, given in Fig. 3, will be utilized for derivation of the rate equations. It can be presented in the

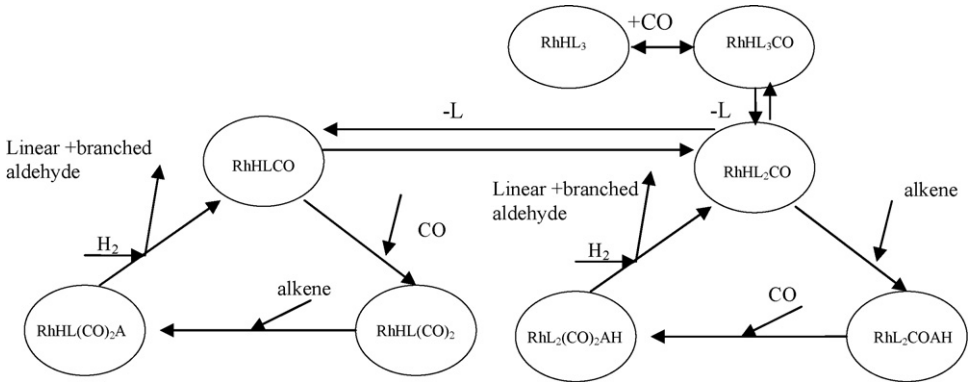

Fig. 3. Hydroformylation mechanism with two cycles.

following form:

	$N^{(1)}$	$N^{(2)}$	$N^{(3)}$	$N^{(4)}$
1. $RhHL_3+CO \Xi RhHL_3CO$	0	0	0	0
2. $RhHL_3CO \Xi RhHL_2CO + L$	0	0	0	0
3. $RhHL_2CO+A \rightarrow RhHL_2COA$	1	0	1	0
4. $RhHL_2COA+CO \rightarrow RhL_2(CO)_2AH$	1	0	1	0
5. $RhL_2(CO)_2AH+H_2 \rightarrow N+ RhHL_2CO$	1	0	0	0
6. $RhL_2(CO)_2AH+H_2 \rightarrow I+ RhHL_2CO$	0	0	1	0
7. $RhHL_2CO \Xi RhHLCO+L$	0	0	0	0
8. $RhHLCO+CO \rightarrow RhHL(CO)_2$	0	1	0	1
9. $RhHL(CO)_2+A \rightarrow RhHL(CO)_2A$	0	1	0	1
10. $RhHL(CO)_2A + H_2 \rightarrow N+RhHLCO$	0	1	0	0
11. $RhHL(CO)_2A + H_2 \rightarrow I+ RhHLCO$	0	0	0	1

$N^{(1)}, N^{(2)}$: $A+CO+H_2=N$, $N^{(3)}, N^{(4)}$: $A+CO+H_2=I$ (4)

The elementary steps above can be described by four reaction routes, *i.e.* sets of stoichiometric numbers of steps. Elementary reactions are grouped in steps, and chemical equations of steps contain reactants and intermediate products. A set of stoichiometric numbers of steps is defined as a reaction route. Routes must be essentially different, and it is impossible to obtain one route through multiplication of another route by a number, although their respective overall equations can be identical. The number of basic routes, P, is determined by $P=S+W-I$, where S is the number of steps, W is the number of balance equations, and I is the number of intermediates. Balance equations determine the relationship between adsorbed intermediates. Such equations can correspond to the total coverage equal to unity. In mechanism (4) A stands for alkene, N and I denote, respectively, linear and branched aldehydes. On the right hand side of equations for the steps stoichiometric numbers along the four routes $N^{(1)}$–$N^{(4)}$ are given. These numbers are selected in a way so that the overall chemical equations do not contain intermediates [6,7].

According to the rule of Horiuti–Temkin, the number of independent routes can be determined by subtracting from the number of steps, equal to 11 in Eq. (4), number of intermediates, equal to 8 {$RhHL_3$, $RhHL_3CO$, $RhHL_2CO$, $RhHL_2COA$, $RhHL_2(CO)_2A$ (note that this is five-coordinated Rh species, similar to the one presented in Fig. 2), RhHLCO, $RhHL(CO)_2$, $RhHL(CO)_2A$} and adding the number of balance equations (here there is one balance equation which is related to the concentration of all rhodium containing intermediates). Following this rule, it can be concluded that there are four independent routes. The first two steps in the mechanism represent so-called hanging vertex, their stoichiometric numbers being equal to zero, and such steps are at steady-state can be considered as quasi-equilibrium ones. Equilibrium step 7 links two catalytic cycles (Fig. 3) together. Mechanism, presented in Eq. (4) is simplified, as it does not distinguish between different geometrical positions (axial or equatorial) of phosphines; however, considerations in the present manuscript are sufficient to describe the kinetic regularities regarding rate and regioselectivity dependencies on the ligand concentrations.

3.1. Derivation of rate equations

Equilibria for steps 1, 2 and 7 give the following equations:

$$C_{RhHL_3CO} = K_1 C_{RhHL_3} P_{CO} \tag{5}$$

$$C_{RhHL_2CO} = \frac{K_1 K_2 C_{RhHL_3} P_{CO}}{C_L} \tag{6}$$

$$C_{RhHLCO} = \frac{K_1 K_2 K_7 C_{RhHL_3} P_{CO}}{C_L^2} \tag{7}$$

In principle rigorous analysis of reaction kinetics requires application of steady-state approximation to steps 3–6 and 8–11 in the reaction mechanism (4). Since the reaction rate displayed first order dependence in the concentrations of alkene, CO and hydrogen [5] according to Eqs. (1) and (2), it is possible to simplify the kinetic analysis and assume that there is only one rate-limiting step in each catalytic route, while the other steps are at quasi-equilibria. Although the rate-determining step in hydroformylation with Rh/PPh_3 systems is not fully understood, it can be assumed that the rate-determining step is H_2 addition in both routes.

It should be noted that an assumption of steady-state for all routes in the cycle does not give a kinetic equation consistent with experimental kinetic regularities.

It holds, therefore, for the intermediate species in the first route that

$$C_{RhHL_2COA} = \frac{K_1 K_2 K_3 C_{RhHL_3} P_{CO} P_A}{C_L} \tag{8}$$

$$C_{RhL_2COAH} = \frac{K_1 K_2 K_3 K_4 C_{RhHL_3} P_{CO}^2 P_A}{C_L} \tag{9}$$

and for the second

$$C_{RhHL(CO)_2} = \frac{K_1 K_2 K_7 K_8 C_{RhHL_3} P_{CO}^2}{C_L^2} \tag{10}$$

$$C_{RhHL(CO)_2A} = \frac{K_1 K_2 K_7 K_8 K_9 C_{RhHL_3} P_{CO}^2 P_A}{C_L^2} \tag{11}$$

The rates along the first and the third routes are expressed by

$$r^{(I)} = r_5 = k_5 P_{H_2} C_{RhL_2(CO)_2AH} = \frac{k_5 K_1 K_2 K_3 K_4 C_{RhHL_3} P_{CO}^2 P_A P_{H_2}}{C_L} \tag{12}$$

$$r^{(III)} = r_6 = k_6 P_{H_2} C_{RhL_2(CO)_2AH} = \frac{k_6 K_1 K_2 K_3 K_4 C_{RhHL_3} P_{CO}^2 P_A P_{H_2}}{C_L} \tag{13}$$

while the rate equations for the second and the fourth routes take a form

$$r^{(II)} = r_{10} = k_{10} P_{H_2} C_{RhHL(CO)_2A} = \frac{k_{10} K_1 K_2 K_7 K_8 K_9 C_{RhHL_3} P_{CO}^2 P_A P_{H_2}}{C_L^2} \tag{14}$$

$$r^{(IV)} = r_{11} = k_{11} P_{H_2} C_{RhHL(CO)_2A} = \frac{k_{11} K_1 K_2 K_7 K_8 K_9 C_{RhHL_3} P_{CO}^2 P_A P_{H_2}}{C_L^2} \tag{15}$$

The balance equation relates all the catalytic intermediate species

$$\begin{aligned} &C_{RhHL_3} + C_{RhHL_3CO} + C_{RhHL_2CO} + C_{RhHLCO} + C_{RhHL_2COA} + C_{RhL_2COAH} \\ &\quad + C_{RhHL(CO)_2} + C_{RhHL(CO)_2A} \\ &= C_{RhHL_3}(1 + K_1 P_{CO} + K_1 K_2 P_{CO}/C_L + K_1 K_2 K_7 P_{CO}/C_L^2 \\ &\quad + K_1 K_2 K_3 P_{CO} P_A/C_L + K_1 K_2 K_3 K_4 P_{CO}^2 P_A/C_L + K_1 K_2 K_7 K_8 P_{CO}^2/C_L^2 \\ &\quad + K_1 K_2 K_7 K_8 K_9 P_{CO}^2 P_A/C_L^2) = C_{Rh}^0 \end{aligned} \tag{16}$$

Combining Eqs. (12), (13) and (16) as well as (14)–(16) the explicit expressions for the reaction rates along the routes are

$$r^{(I)} = \frac{k_5K_1K_2K_3K_4P_{CO}^2P_AP_{H_2}/C_L}{1+K_1P_{CO}+K_1K_2P_{CO}/C_L+K_1K_2K_7P_{CO}/C_L^2+K_1K_2K_3P_{CO}P_A/C_L+K_1K_2K_3K_4P_{CO}^2P_A/C_L+K_1K_2K_7K_8P_{CO}^2/C_L^2+K_1K_2K_7K_8K_9P_{CO}^2P_A/C_L^2}C_{Rh}^0 \quad (17)$$

$$r^{(III)} = \frac{k_6K_1K_2K_3K_4P_{CO}^2P_AP_{H_2}/C_L}{1+K_1P_{CO}+K_1K_2P_{CO}/C_L+K_1K_2K_7P_{CO}/C_L^2+K_1K_2K_3P_{CO}P_A/C_L+K_1K_2K_3K_4P_{CO}^2P_A/C_L+K_1K_2K_7K_8P_{CO}^2/C_L^2+K_1K_2K_7K_8K_9P_{CO}^2P_A/C_L^2}C_{Rh}^0 \quad (18)$$

$$r^{(II)} = \frac{k_{10}K_1K_2K_7K_8K_9P_{CO}^2P_AP_{H_2}/C_L^2}{1+K_1P_{CO}+K_1K_2P_{CO}/C_L+K_1K_2K_7P_{CO}/C_L^2+K_1K_2K_3P_{CO}P_A/C_L+K_1K_2K_3K_4P_{CO}^2P_A/C_L+K_1K_2K_7K_8P_{CO}^2/C_L^2+K_1K_2K_7K_8K_9P_{CO}^2P_A/C_L^2}C_{Rh}^0 \quad (19)$$

$$r^{(IV)} = \frac{k_{11}K_1K_2K_7K_8K_9P_{CO}^2P_AP_{H_2}/C_L^2}{1+K_1P_{CO}+K_1K_2P_{CO}/C_L+K_1K_2K_7P_{CO}/C_L^2+K_1K_2K_3P_{CO}P_A/C_L+K_1K_2K_3K_4P_{CO}^2P_A/C_L+K_1K_2K_7K_8P_{CO}^2/C_L^2+K_1K_2K_7K_8K_9P_{CO}^2P_A/C_L^2}C_{Rh}^0 \quad (20)$$

The first order in CO and alkene indicates that in denominator unity as well as terms containing P_{CO}^2 and P_A can be neglected, which gives

$$r^{(I)} = \frac{k_5K_2K_3K_4P_{CO}P_AP_{H_2}/C_L}{1+K_2/C_L+K_2K_7/C_L^2}C_{Rh}^0,$$
$$r^{(III)} = \frac{k_6K_2K_3K_4P_{CO}P_AP_{H_2}/C_L}{1+K_2/C_L+K_2K_7/C_L^2}C_{Rh}^0 \quad (21)$$

$$r^{(II)} = \frac{k_{10}K_2K_7K_8K_9P_{CO}P_AP_{H_2}/C_L^2}{1+K_2/C_L+K_2K_7/C_L^2}C_{Rh}^0,$$
$$r^{(IV)} = \frac{k_{11}K_2K_7K_8K_9P_{CO}P_AP_{H_2}/C_L^2}{1+K_2/C_L+K_2K_7/C_L^2}C_{Rh}^0 \quad (22)$$

The generation rates for the components are written as follows:

$$r_N = r^{(I)} + r^{(II)} = \frac{k_5K_2K_3K_4P_{CO}P_AP_{H_2}/C_L + k_{10}K_2K_7K_8K_9P_{CO}P_AP_{H_2}/C_L^2}{1+K_2/C_L+K_2K_7/C_L^2}C_{Rh}^0 = \frac{k_5K_3K_4/K_7P_{CO}P_AP_{H_2}C_L + k_{10}K_8K_9P_{CO}P_AP_{H_2}}{1+C_L/K_7+C_L^2/K_2K_7}C_{Rh}^0 \quad (23)$$

$$r_I = r^{(III)} + r^{(IV)} = \frac{k_6K_3K_4/K_7P_{CO}P_AP_{H_2}C_L + k_{11}K_8K_9P_{CO}P_AP_{H_2}}{1+C_L/K_7+C_L^2/K_2K_7}C_{Rh}^0 \quad (24)$$

Eq. (23) could be modified

$$r_N = \frac{k_5K_3K_4/K_7P_{CO}P_AP_{H_2}C_L(1+(k_{10}K_7K_8K_9/k_5K_3K_4))}{1+C_L/K_7+C_L^2/K_2K_7}C_{Rh}^0 = \frac{kP_pP_{H_2}P_{CO}(1+k'C_L)}{1+aC_L+bC_L^2}C_{Rh}^0 \quad (25)$$

with

$$k = \frac{k_5K_3K_4}{K_7}, \qquad k' = \frac{k_{10}K_7K_8K_9}{k_5K_3K_4} \quad a = \frac{1}{K_7}, \quad b = \frac{1}{K_2K_7} \quad (26)$$

Analogously the generation rate for the branched aldehyde is obtained

$$r_i = \frac{k_6K_3K_4/K_7P_{CO}P_AP_{H_2}C_L(1+(k_{11}K_7K_8K_9/k_6K_3K_4))}{1+aC_L+bC_L^2}C_{Rh}^0 = \frac{kP_pP_{H_2}P_{CO}(k''+k'''C_L)}{1+aC_L+bC_L^2}C_{Rh}^0 \quad (27)$$

where

$$k'' = \frac{k_6}{k_5} \quad \text{and} \quad k''' = k'\frac{k_{11}}{k_{10}} = \frac{k_{11}K_7K_8K_9}{k_5K_3K_4} \quad (28)$$

Analysis of Eqs. (25) and (27) shows that the reaction rate is first order in CO, alkene and hydrogen in agreement with experimental data and that an order in the ligand concentration is negative in agreement with experimental observations [5]. Regioselectivity (the ratio between linear and branched aldehyde) has the following dependence on the ligand concentration:

$$rs = \frac{r_n}{r_i} = \frac{1+k'C_L}{k''+k'''C_L} \quad (29)$$

When it is compared with the empirical power law dependence (Eq. (3)) $rs \sim C_{PPh_3}^{0.16}$, it is clear that the term in denominator containing $k'''C_L$ could be neglected. Additionally graphical comparison between the power law dependence and Eq. (29) given in Fig. 4 suggests that $k'' = k_6/k_5 \approx 1$ at non-negligible ligand concentration, which means that the cycle involving RhHLCO is not regioselective, providing an equimolar ratio of linear and branched aldehyde.

These simplifications finally lead to the following equations:

$$r_i = \frac{kP_pP_{H_2}P_{CO}}{1+aC_L+bC_L^2}C_{Rh}^0, \qquad r_n = \frac{kP_pP_{H_2}P_{CO}(1+k'C_L)}{1+aC_L+bC_L^2}C_{Rh}^0 \quad (30)$$

which were used for data fitting.

3.2. Data fitting

In order to elucidate the applicability of the kinetic model, described above, the system of Eq. (30) was solved numerically in the parameter estimations with the backward difference method by minimization of the sum of residual squares with non-linear regression using the simplex and Levenberg–Marquardt optimization algorithms implemented in the software Modest [8].

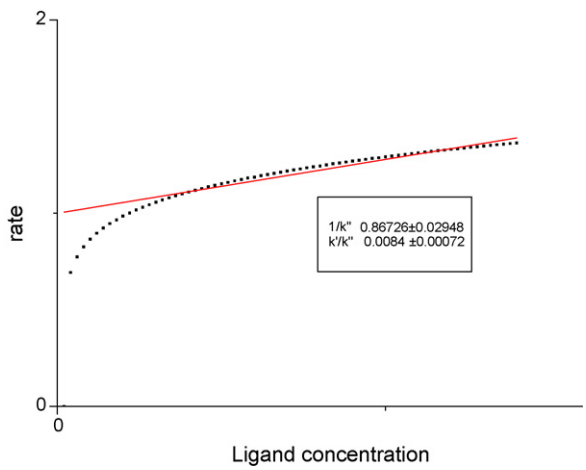

Fig. 4. Comparison between Eqs. (3) and (29) for $k'''C_L \approx 0$.

Table 1
Values of the estimated parameters.

Parameter	Estimated value	Est. relative standard error (%)
A_1	0.21×10^2	12.1
A_2	0.11×10^3	23.0
a	75.8	4.0
b	2650	9.7
E_{a1}	0.76×10^5	25.9

Note: Dimensions: $[E_a]$ = J mol^{-1}, $[A_1]$ = dm^8 mol^{-2} min^{-1}, and $[A_2]$ = dimensionless.

Eq. (30) was in fact modified to include concentrations of alkene, hydrogen and CO:

$$r_i = \frac{kC_pC_{H_2}C_{CO}}{1 + aC_L + bC_L^2}C_{Rh}^0, \qquad r_n = \frac{kC_pC_{H_2}C_{CO}(1 + k'C_L)}{1 + aC_L + bC_L^2}C_{Rh}^0 \tag{31}$$

In Eq. (31) C_P (mol/dm^3), C_{H_2} (mol/dm^3), C_{CO} (mol/dm^3), $[Rh]$ (mass fraction), and $[L]$ (mass fraction) denote concentration of propene, concentration of hydrogen and carbon monoxide, mass fraction of rhodium, and mass fraction of ligand, respectively. The solubility of hydrogen and carbon monoxide was studied previously [9]:

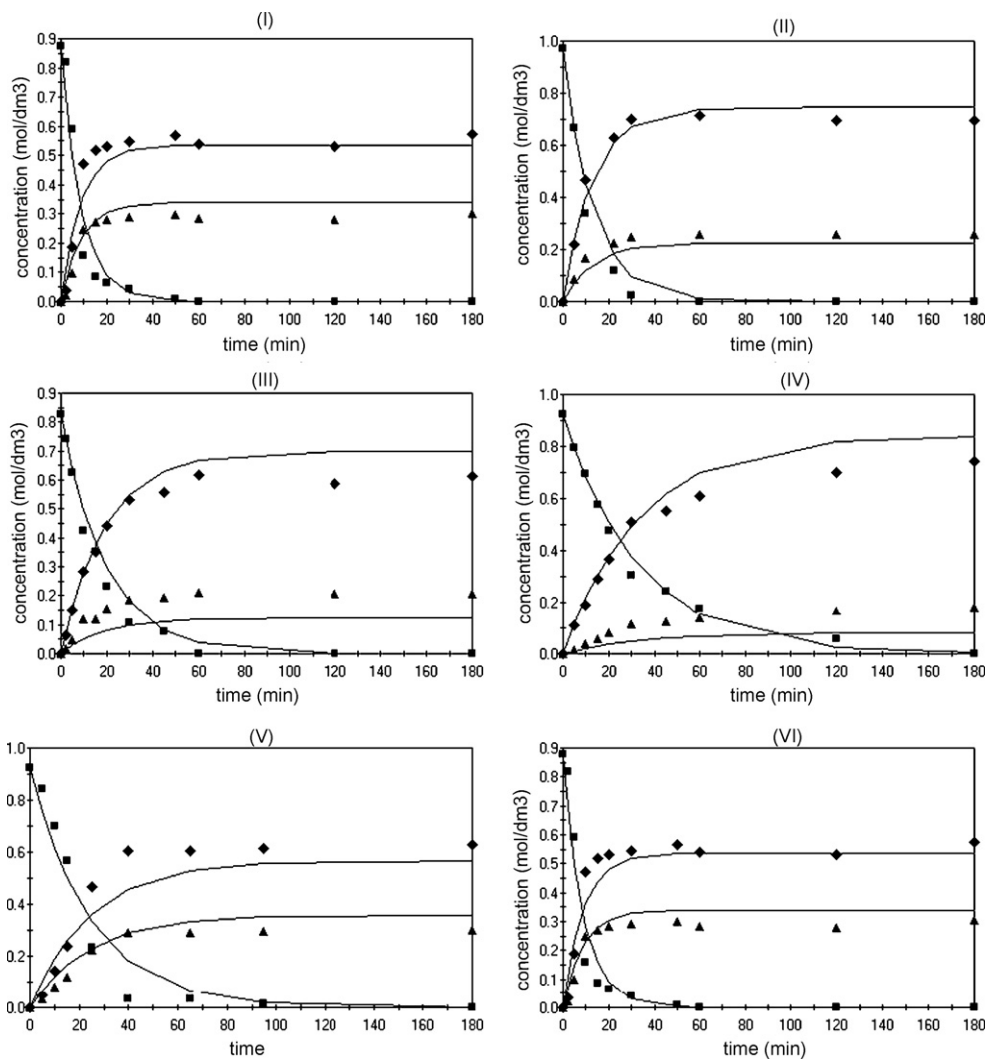

Fig. 5. Comparison between experimental and calculated data at some selected. Solid line: predicted value, ■: propene, ▲: isomeric aldehyde, and ♦: normal aldehyde. Conditions: reactant, 1.2 bar overpressure of propene at 25 °C (approx. 0.15 mol); solvent, 150 ml of 2,2,4-trimethyl-1,3-pentanediol monoisobutyrate; metal precursor, (acetylacetonato)dicarbonylrhodium(I); rhodium concentration, 100 ppm; H_2-to-CO ratio, 1:1; reaction time, 180 min. The reaction temperature, pressure of CO and H_2, and ligand concentration was varied as follows. (I) T = 100 °C, P_{H_2} = 5.5 bar, P_{CO} = 5.5 bar, C_L = 0.005 (mass); (II) T = 100 °C, P_{H_2} = 5.5 bar, P_{CO} = 5.5 bar, C_L = 0.02; (III) T = 100 °C, P_{H_2} = 5.5 bar, P_{CO} = 5.5 bar, C_L = 0.04; (IV) T = 100 °C, P_{H_2} = 5.5 bar, P_{CO} = 5.5 bar, C_L = 0.08; (V) T = 85 °C, P_{H_2} = 5.5 bar, P_{CO} = 5.5 bar, C_L = 0.005; (VI) T = 100 °C, P_{H_2} = 5.5 bar, P_{CO} = 5.5 bar, C_L = 0.005;.

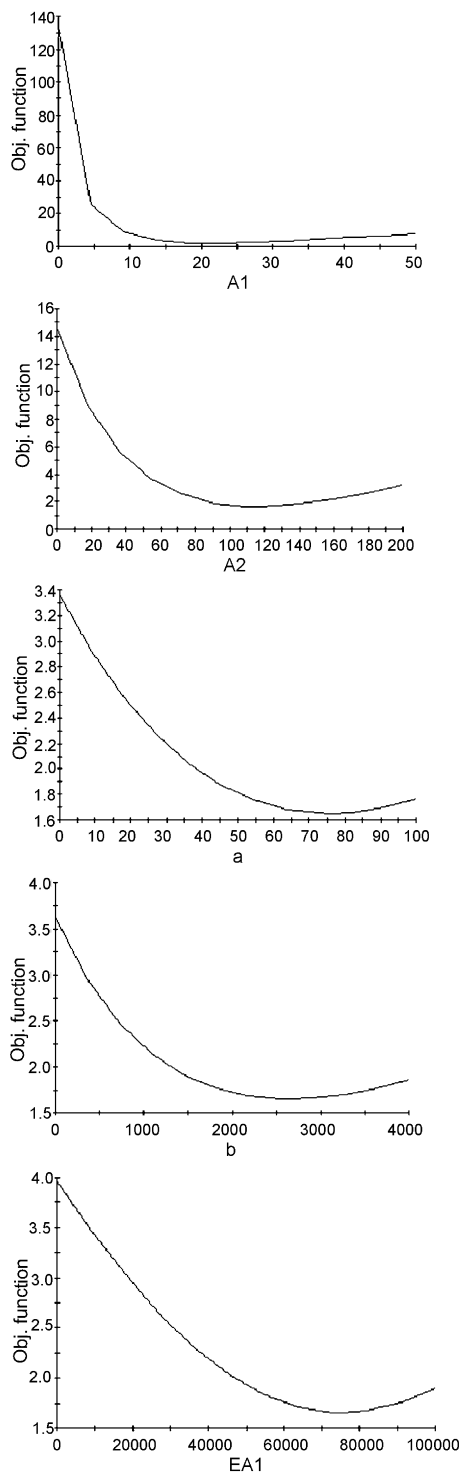

Fig. 6. Objective function vs. kinetic parameters.

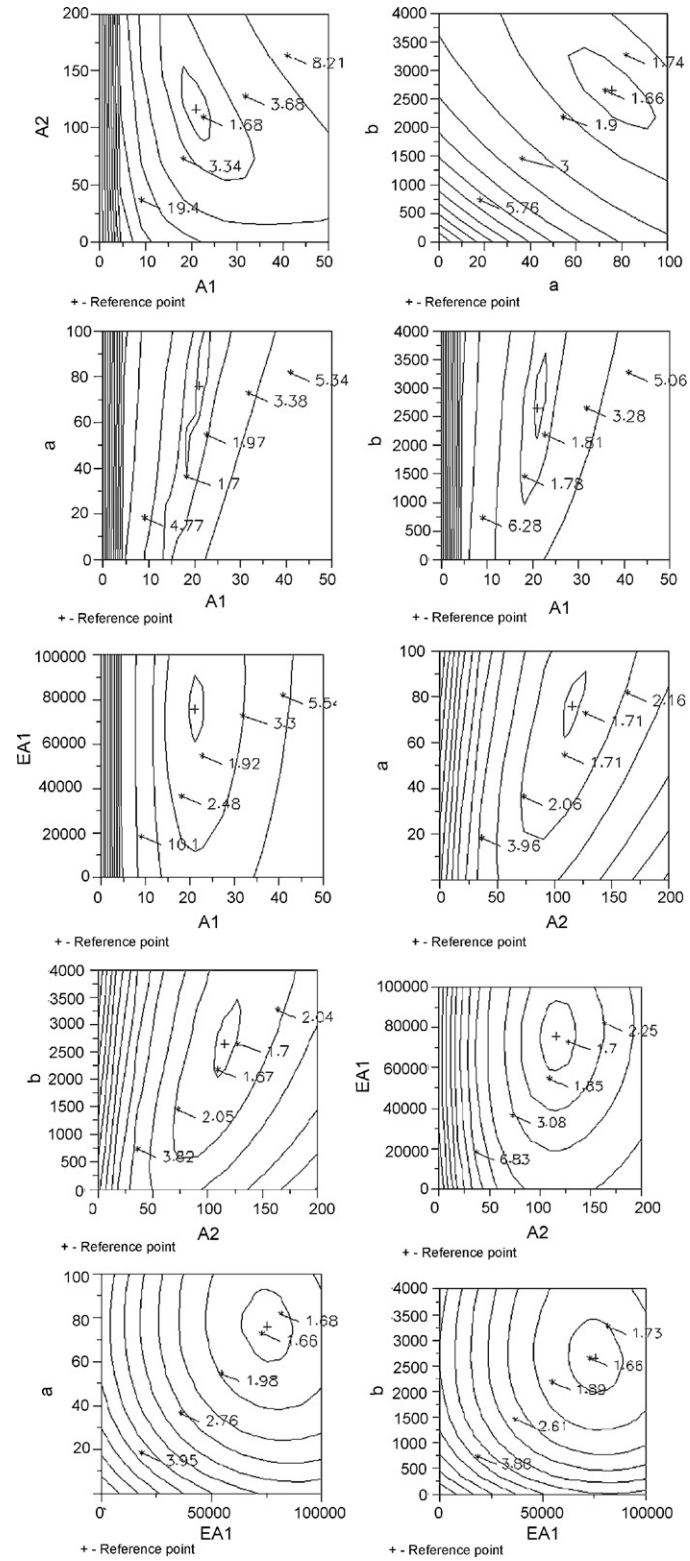

Fig. 7. Contour plots: A_2 vs. A_1, b vs. a, a vs. A_1, b vs. A_1, E_{A_1} vs. A_1, a vs. A_2, b vs. A_2, E_{A_1} vs. A_2, a vs. E_{A_1}, and b vs. E_{A_1}.

The lumped kinetic constant k was assumed to follow the Arrhenius dependence:

$$k = A \exp\left(-\frac{E_a}{R}\left(\frac{1}{T} - \frac{1}{T_{mean}}\right)\right) \tag{32}$$

where A, E_a, T and T_{mean} denote frequency factor, activation energy, the gas constant, reaction temperature and mean temperature of the experiments, respectively.

It was observed experimentally that regioselectivity did not show any dependence on T [5] in the studied temperature range, therefore the lumped constant k' was set to be temperature independent. The model is still over-parametrized and could be further simplified by assuming negligible temperature dependences of equilibrium constants, which means in other words independence of parameters a and b on temperature.

The sum of squares in the parameter estimation was minimized using a step size of 0.1 and 1×10^{-6} for the absolute and relative tolerances of the simplex and Levenberg–Marquardt optimizer, starting with the former method and changing to the latter one while approaching the minimum.

Comparison between estimated and calculated values is given in Fig. 5, showing very good description of the data. The degree of explanation was 94% and sum of residuals was 1.65. The values of the estimated parameters, the estimated relative standard errors (in %) are shown in Table 1.

The value of activation energy for hydroformylation for Rh complexes was reported to be 71 kJ/mol for octene [10], and 116 kJ/mol for hexene [11], while for propene the value of activation energies for hydroformylation with supported ionic liquid phase catalyst was 63 kJ/mol [12], which is very close to the theoretical values [4] as well as those experimentally obtained in the present study.

The table demonstrates that the parameters are well identified. The objective function $SRS = l(\theta) = \left\| y - y_p \right\|_w^2 = \sum_{k=1}^{nsets} \sum_{j=1}^{nobs(k)} \sum_{i=1}^{nydata(j,k)} (y_{ijk} - y_{pijk})^2 w_{ijk}$ dependence for the parameters is given in Fig. 6, while Fig. 7 displays contour plots, proposing that there is practically no correlation between parameters.

4. Conclusions

Experimental data on propene hydroformylation to linear and branched aldehydes with rhodium triphenylphosphine catalyst were obtained by varying hydrogen and CO partial pressure and were compared with a mechanistic model. The reaction orders in hydrogen, CO and alkene are equal to unity. The regioselectivity was independent on the concentration of reactants, specifically that of carbon monoxide, displaying minor dependence on the ligand concentration.

The mechanism for alkenes hydroformylation was proposed in accordance with literature data and experimental observations in order to account for kinetics of this reaction. The reaction network was supposed to contain two mechanistically different cycles, each of them could in principle lead to linear and branched products. Kinetic hypothesis allowed some simplifications, in particular that one cycle is selective to linear aldehydes, while the second one gives stoichiometric amounts of linear and branched products. A complicated mechanism involving different intermediates was translated into tractable rate expressions. Numerical data fitting was performed and it was concluded that the advanced kinetic model, based on mechanistic considerations, describes well experimental data, in particular regioselectivity. At the same time it should be noted that the general kinetic scheme was somewhat simplified while deriving kinetic equations by assuming one rate-determining step in each catalytic route, which was justified by the obtained kinetic regularities. For more complicated kinetics, these simplifications could be relaxed.

Acknowledgements

This work is a part of activities with Process Chemistry Centre (2000–2011) by Academy of Finland. The authors are grateful to Professor Dieter Vogt (Eindhoven University of Technology) for many useful comments and suggestions.

References

[1] P.W.N.M. Van Leeuwen, C. Claver, Rhodium Catalyzed Hydroformylation, Kluwer Academic Publishers, Dordrecht, Netherlands, 2000;
J. Falbe, New Syntheses with Carbon Monoxide, Springer Verlag, Berlin, 1980;
M. Torrent, M. Sola, G. Frenking, Chem. Rev. 100 (2000) 439.
[2] M. Beller, B. Cornils, C.D. Frohning, C.W. Kohlpaintner, J. Mol. Catal. A 104 (1995) 17.
[3] J.A. Moulijn, M. Makkee, A. van Diepen, Chemical Process Technology, Wiley, Chichester, 2001.
[4] E. Zuidema, E. Daura-Oller, J.J. Carbo, C. Bo, P.W.N.M. Leeuwen, Organometallics 26 (2007) 2234.
[5] A. Bernas, P. Mäki-Arvela, J. Lehtonen, T. Salmi, D.Yu. Murzin, Ind. Eng. Chem. Res. 47 (2008) 4317.
[6] M.I. Temkin, Adv. Catal. 28 (1979) 173.
[7] D.Yu. Murzin, T. Salmi, Catalytic Kinetics, Elsevier, Amsterdam, 2005.
[8] H. Haario, Modest User's Guide, Profmath, Helsinki, 2001.
[9] C. Still, T. Salmi, P. Mäki-Arvela, K. Eränen, D.Yu. Murzin, J. Lehtonen, Chem. Eng. Sci. 61 (2006) 3698.
[10] U.J. Jáuregui-Haza, E. Pardillo-Fontdevila, Ph. Kalck, A.M. Wilhelm, H. Delmas, Catal. Today 79–80 (2003) 409.
[11] R.M. Deshpande, R.V. Chaudhari, Ind. Eng. Chem. Res. 27 (1988) 1996.
[12] A. Riisager, R. Fehrmann, M. Haumann, B.S.K. Gorle, P. Wasserscheid, Ind. Eng. Chem. Res. 44 (2005) 9853.